

# Josephson current in ballistic heterostructures with spin-active interfaces

Mikhail S. Kalenkov and Artem V. Galaktionov

*I.E. Tamm Department of Theoretical Physics, P.N. Lebedev Physics Institute, 119991 Moscow, Russia*

Andrei D. Zaikin

*Forschungszentrum Karlsruhe, Institut für Nanotechnologie, 76021, Karlsruhe, Germany and  
I.E. Tamm Department of Theoretical Physics, P.N. Lebedev Physics Institute, 119991 Moscow, Russia*

We develop a general microscopic theory of dc Josephson effect in hybrid SNS structures with ballistic electrodes and spin-active NS interfaces. We establish a direct relation between the spectrum of Andreev levels and the Josephson current which contains complete information about non-trivial interplay between Andreev reflection and spin-dependent interface scattering. The system exhibits a rich structure of properties sensitive to spin-dependent barrier transmissions, spin-mixing angles, relative magnetization orientation of interfaces and the kinematic phase of scattered electrons. We analyze the current-phase relations and identify the conditions for the presence of a  $\pi$ -junction state in the systems under consideration. We also analyze resonant enhancement of the supercurrent in gate-voltage-driven nanojunctions. As compared to the non-magnetic case, this effect can be strongly modified by spin-dependent scattering at NS interfaces.

## I. INTRODUCTION

Spin-sensitive Andreev reflection in superconducting hybrid structures yields a number of interesting and non-trivial effects which have been addressed and studied in the literature. Already more than three decades ago it was realized that spin-flip electron tunneling through a magnetic interface between two superconductors may cause a sign change of the Josephson current and yield the so-called  $\pi$ -junction state in superconducting weak links<sup>1</sup>. The same effect can also occur in superconductor-ferromagnet-superconductor (SFS) junctions where the Josephson critical current was predicted to oscillate as a function of the ferromagnet layer thickness also leading to formation of the  $\pi$ -junction state<sup>2,3</sup>. These theoretical predictions were confirmed in experiments with SFS junctions<sup>4,5</sup>.

More recently it was realized<sup>6,7</sup> that the Cooper pair wave function in SF hybrids may change its symmetry from a singlet in a superconductor to a triplet in a ferromagnet. This so-called odd-frequency pairing state<sup>6</sup> implies that Cooper pairs can penetrate deep into the ferromagnet thus causing the long range proximity effect in SF systems. Experimental evidence for such long range coherent behavior of SF hybrids was discussed in Ref. 8.

Another interesting realization of this long range proximity effect is the possibility for non-vanishing Josephson current to flow across superconducting weak links containing strong ferromagnets or the so-called half-metals (H). Note that spin-singlet Cooper pairs cannot penetrate into H-metals because such metals are fully spin polarized materials acting as insulators for electrons with one of the two spin directions. Hence, no supercurrent carried by spin-singlet Cooper pairs can occur in SHS junctions. Superconducting correlations can nevertheless survive deep inside strong ferromagnets provided there exists a mechanism for spin-flip scattering at both HS

interfaces of the junction. This mechanism allows for conversion of spin-singlet pairing in S-electrodes into spin-triplet pairing in H-metals thus making it possible for the supercurrent to flow across the system. A theory of this non-trivial Josephson effect in SHS junctions was recently addressed by a number of authors<sup>9,10,11</sup>. Experimental results<sup>12</sup> appear to support that non-vanishing supercurrent can indeed flow across sufficiently thick SHS junctions.

The main goal of this paper is to develop a general theory of dc Josephson effect in SNS heterostructures with spin-active interfaces. Previously<sup>13</sup> we already demonstrated that spin-dependent scattering at such interfaces yields a number of interesting and non-trivial properties of non-local Andreev reflection in three-terminal NSN devices. Here we find that both the Josephson critical current and the current-phase relation in SNS junctions are very sensitive to particular values of (a) spin-dependent interface transmissions, (b) spin-mixing angles and (c) the electron kinematic phase showing a rich variety of features which can be detected and studied in future experiments.

One possible experimental realization of SNS junctions with spin-active interfaces is achieved by placing a thin layer of some magnetic material at the interfaces between superconducting and normal metals. In this case transmission probabilities for spin-up and spin-down electrons propagating through such interfaces may take different values. In addition, the scattering phase of incoming electrons may also depend on their spin states. This physical situation can be modelled by a spin-active interface described by two (spin-up and spin-down) transmission probabilities and by the so-called spin-mixing angle which is just the difference between the scattering phases for the spin-up and spin-down states of incoming electrons. Yet one more parameter – the kinematic phase – should be introduced in order to account for the phase acquired by an electron between successive scattering events at NS interfaces. This phase is essentially set

by the product of the Fermi momentum and the distance covered by an electron between two scattering events. Since the electron momentum can be controlled (shifted) by applying the gate voltage the system can be periodically driven to and out of resonance thereby rendering a possibility to experimentally investigate the dependence of the Josephson current on the kinematic phase.

The structure of the paper is as follows. In Sec. 2 we will define our model and specify some key equations that will be employed in our further consideration. Sec. 3 is devoted to the analysis of Andreev bound states in SNS junctions with spin-active interfaces. In Sec. 4 we will demonstrate that the Josephson current in our structure can be directly expressed in terms of the Andreev spectrum and derive the general expression for this current. This expression will then be analyzed in Sec. 5 in a number of interesting limits. In Sec. 6 we will briefly summarize our main observations. Some technical details of our analysis will be presented in Appendices A and B.

## II. THE MODEL AND BASIC EQUATIONS

For our analysis we will employ the standard model of a planar ballistic SNS junction (Fig. 1) with spin-active NS interfaces (located at  $x = d_1$  and  $x = d_2$ ) and cross-section area  $\mathcal{A}$ . Outside an immediate vicinity of the interface regions quasiparticle wave functions can be represented as a sum of two rapidly oscillating exponents

$$\Psi = \Psi_+(x)e^{ip_{Fx}x + i\mathbf{p}_\parallel \boldsymbol{\rho}} + \Psi_-(x)e^{-ip_{Fx}x + i\mathbf{p}_\parallel \boldsymbol{\rho}}, \quad (1)$$

where  $x$  is coordinate normal to the NS interfaces,  $\boldsymbol{\rho}$  represents the coordinates in the transversal directions and  $p_{Fx} = \sqrt{p_F^2 - \mathbf{p}_\parallel^2} > 0$  is the normal component of the Fermi momentum. The wave functions  $\Psi_\pm(x)$  vary smoothly at atomic distances. Applying the standard Andreev approximation it is easy to demonstrate that  $\Psi_\pm(x)$  obeys the following equation

$$\left[ \varepsilon \pm i\tau_3 v_{Fx} \frac{\partial}{\partial x} - \begin{pmatrix} 0 & i\sigma_2 \Delta(x) \\ -i\sigma_2 \Delta(x)^* & 0 \end{pmatrix} \right] \Psi_\pm = 0, \quad (2)$$

where  $\hat{\tau}_3$  is the Pauli matrix in the Nambu space,  $\sigma_i$  are the Pauli matrices in the spin space,  $v_{Fx} = p_{Fx}/m$  and  $\Delta$  is the BCS order parameter which is assumed to be spatially constant equal to  $|\Delta_1|e^{-i\chi/2}$  ( $|\Delta_2|e^{i\chi/2}$ ) in the first (second) superconducting electrode and is set equal to zero  $\Delta = 0$  in the normal metal. Eq. (2) does not apply at the interfaces and should be supplemented by the proper boundary conditions which account for spin-sensitive electron scattering. In order to formulate these boundary conditions we will employ the general  $S$ -matrix formalism. For instance, matching of the quasiparticle wave functions at the first interface is performed with the aid of the following equation

$$\begin{pmatrix} \Psi_{1-} \\ \Psi_{1'+} \end{pmatrix} = \begin{pmatrix} \hat{S}_{11} & \hat{S}_{11'} \\ \hat{S}_{1'1} & \hat{S}_{1'1'} \end{pmatrix} \begin{pmatrix} \Psi_{1+} \\ \Psi_{1'-} \end{pmatrix}. \quad (3)$$

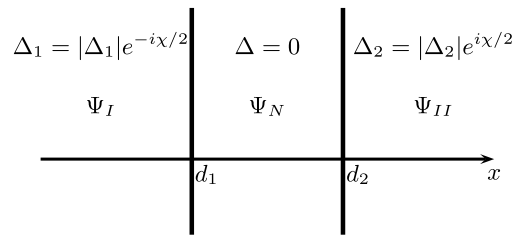


FIG. 1: SNS junction with spin-active interfaces located at  $x = d_1$  and  $x = d_2$ .

Here  $\Psi_{1+}$ ,  $\Psi_{1-}$  and  $\Psi_{1'+}$ ,  $\Psi_{1'-}$  are the quasiparticle wave function amplitudes respectively at superconducting and normal sides of the first interface. The matrices  $\hat{S}_{ij}$  are diagonal in the Nambu space

$$\hat{S}_{ij} = \begin{pmatrix} S_{ij} & 0 \\ 0 & \underline{S}_{ij} \end{pmatrix}, \quad (4)$$

where  $S_{ij}$  and  $\underline{S}_{ij}$  are the building blocks of the full electron and hole interface  $S$ -matrices<sup>16</sup>

$$S_1 = \begin{pmatrix} S_{11} & S_{11'} \\ S_{1'1} & S_{1'1'} \end{pmatrix}, \quad \underline{S}_1 = \begin{pmatrix} \underline{S}_{11} & \underline{S}_{11'} \\ \underline{S}_{1'1} & \underline{S}_{1'1'} \end{pmatrix}, \quad (5)$$

$$S_1 S_1^+ = 1, \quad \underline{S}_1 \underline{S}_1^+ = 1. \quad (6)$$

In general electron and hole  $S$ -matrices do not coincide with each other but obey the following relation

$$\underline{S}_1(\mathbf{p}_\parallel) = S_1^T(-\mathbf{p}_\parallel). \quad (7)$$

Electron scattering at the second interface is described analogously with the aid of the matrices  $S_2$  and  $\underline{S}_2$  which have the same structure as in Eqs. (5)-(7).

## III. ANDREEV STATES

With aid of the above equations it is convenient to analyze the spectrum of Andreev bound states in SNS heterostructures with spin active interfaces. For this purpose it is necessary to solve Eq. (2) and explicitly find quasiparticle wave functions of our system. In the first superconductor  $x < d_1$  the wave function has the form

$$\Psi_I = \begin{pmatrix} -i\sigma_2 e^{-i\chi/2} a_1 A_1 \\ A_1 \end{pmatrix} e^{ip_{Fx}(x-d_1)} e^{\kappa_1(x-d_1)} + \begin{pmatrix} A_2 \\ i\sigma_2 e^{i\chi/2} a_1 A_2 \end{pmatrix} e^{-ip_{Fx}(x-d_1)} e^{\kappa_1(x-d_1)}, \quad (8)$$

where  $\kappa_m = \sqrt{|\Delta_m|^2 - \varepsilon^2}/v_{Fx}$  and  $a_m = (-\varepsilon + \sqrt{\varepsilon^2 - |\Delta_m|^2})/|\Delta_m|$  ( $m = 1, 2$ ). The functions  $a_m(\varepsilon)$  are analytic in the upper half-plane of the complex variable  $\varepsilon$ . For real  $\varepsilon$  they read

$$a_m(\varepsilon) = \begin{cases} \frac{-\varepsilon + i\sqrt{|\Delta_m|^2 - \varepsilon^2}}{|\Delta_m|}, & |\varepsilon| < |\Delta_m|, \\ \frac{-\varepsilon + \sqrt{\varepsilon^2 - |\Delta_m|^2} \operatorname{sgn}(\varepsilon)}{|\Delta_m|}, & |\varepsilon| > |\Delta_m|, \end{cases} \quad (9)$$

while for purely imaginary values of  $\varepsilon$  we have

$$a_m(i\omega) = i \frac{\sqrt{\omega^2 + |\Delta_m|^2} - \omega}{|\Delta_m|}, \quad \omega > 0. \quad (10)$$

In the normal metal  $d_1 < x < d_2$  and in the second superconductor  $x > d_2$  one has respectively

$$\begin{aligned} \Psi_N = & \left( \begin{array}{c} e^{i\varepsilon(x-d_1)/v_{Fx}} B_1 \\ e^{-i\varepsilon(x-d_1)/v_{Fx}} B_2 \end{array} \right) e^{ip_{Fx}(x-d_1)} + \\ & + \left( \begin{array}{c} e^{-i\varepsilon(x-d_1)/v_{Fx}} B_3 \\ e^{i\varepsilon(x-d_1)/v_{Fx}} B_4 \end{array} \right) e^{-ip_{Fx}(x-d_1)} \end{aligned} \quad (11)$$

and

$$\begin{aligned} \Psi_{II} = & \left( \begin{array}{c} C_1 \\ i\sigma_2 e^{-i\chi/2} a_2 C_1 \end{array} \right) e^{ip_{Fx}(x-d_2)} e^{-\kappa_2(x-d_2)} + \\ & + \left( \begin{array}{c} -i\sigma_2 e^{i\chi/2} a_2 C_2 \\ C_2 \end{array} \right) e^{-ip_{Fx}(x-d_2)} e^{-\kappa_2(x-d_2)}. \end{aligned} \quad (12)$$

All coefficients  $A_{1,2}$ ,  $B_{1,2,3,4}$  and  $C_{1,2}$  are vectors in the spin space which should be determined from the match-

ing conditions at both NS interfaces. From Eq. (3) at the first interface ( $x = d_1$ ) we obtain

$$A_2 = S_{11}(-i\sigma_2 a_1 e^{-i\chi/2}) A_1 + S_{11'} B_3, \quad (13)$$

$$(i\sigma_2 a_1 e^{i\chi/2}) A_1 = \underline{S}_{11} A_1 + \underline{S}_{11'}^+ B_4, \quad (14)$$

$$B_1 = S_{1'1}(-i\sigma_2 a_1 e^{-i\chi/2}) A_1 + S_{1'1'} B_3, \quad (15)$$

$$B_2 = \underline{S}_{1'1} A_1 + \underline{S}_{1'1'} B_4. \quad (16)$$

These equations yield the relation between the amplitudes for the incoming and outgoing electron and hole waves (respectively  $B_3$ ,  $B_4$  and  $B_1$ ,  $B_2$ ):

$$\begin{pmatrix} B_1 \\ B_2 \end{pmatrix} = K_1 \begin{pmatrix} B_3 \\ B_4 \end{pmatrix}, \quad (17)$$

where  $K_1$  is the scattering matrix which describes both normal and Andreev reflection at the first interface. This matrix has the form

$$K_1 = \begin{pmatrix} S_{1'1'} + a_1^2 S_{1'1} \sigma_2 (\underline{S}_{11} - a_1^2 \sigma_2 S_{11} \sigma_2)^{-1} \sigma_2 S_{11'} & ia_1 e^{-i\chi/2} S_{1'1} \sigma_2 (\underline{S}_{11} - a_1^2 \sigma_2 S_{11} \sigma_2)^{-1} \underline{S}_{11'} \\ ia_1 e^{i\chi/2} \underline{S}_{1'1} (\underline{S}_{11} - a_1^2 \sigma_2 S_{11} \sigma_2)^{-1} \sigma_2 S_{11'} & \underline{S}_{1'1'} - \underline{S}_{1'1} (\underline{S}_{11} - a_1^2 \sigma_2 S_{11} \sigma_2)^{-1} \underline{S}_{11'} \end{pmatrix} \quad (18)$$

Diagonal blocks of this matrix describes electron-electron and hole-hole amplitudes while off-diagonal blocks account for electron-hole conversion. One can directly verify that the matrix  $K_1$  is unitary for subgap energies  $|\varepsilon| < |\Delta_1|$  at which no excitations exist in the superconducting electrode I.

Analogously from the matching conditions at the second interface ( $x = d_2$ ) we obtain

$$\begin{pmatrix} B_3 \\ B_4 \end{pmatrix} = e^{-i\varphi} Q K_2 Q \begin{pmatrix} B_1 \\ B_2 \end{pmatrix}, \quad (19)$$

where  $K_2$  is scattering matrix for the second interface at subgap energies  $|\varepsilon| < |\Delta_2|$  and we introduced the following notations

$$e^{2ip_{Fx}(d_2-d_1)} = e^{-i\varphi}, \quad e^{-i\varepsilon(d_2-d_1)/v_{Fx}} = q^2. \quad (20)$$

The matrix  $K_2$  is defined by Eq. (18) with  $1 \rightarrow 2$  and  $\chi \leftrightarrow -\chi$ . The transfer matrix  $Q$  has a simple diagonal structure

$$Q = \begin{pmatrix} q^{-2} \sigma_0 & 0 \\ 0 & q^2 \sigma_0 \end{pmatrix}. \quad (21)$$

It provides the relations between  $\Psi_{\pm}$ -amplitudes at both NS interfaces (on the normal metal side):

$$\Psi_{N+}(d_2) = Q^{-1} \Psi_{N+}(d_1), \quad (22)$$

$$\Psi_{N-}(d_2) = Q \Psi_{N-}(d_1). \quad (23)$$

Combining Eqs. (17) and (19) we obtain the following general condition which defines the energies of Andreev bound states in our system:

$$P(\varepsilon, \mathbf{p}_{\parallel}, \chi) = \det |1 - e^{-i\varphi} Q K_2 Q K_1| = 0 \quad (24)$$

Note that scattering properties of the first (second) interface enter into  $P$  only through the matrix  $K_1$  ( $K_2$ ) while the transfer matrix  $Q$  and the kinematic phase  $\varphi$  determine the dependence of the bound state energy on the thickness of the normal metal layer  $d = d_2 - d_1$ . It is also worth pointing out that our Eq. (24) can be rewritten in terms of the effective energy dependent scattering matrix<sup>14,15</sup>

$$\begin{aligned} P_1(\varepsilon, \mathbf{p}_{\parallel}, \chi) = \\ = \det |\underline{S}(\mathbf{p}_{\parallel}, \varepsilon) - A(\varepsilon, \chi) \mathcal{S}(\mathbf{p}_{\parallel}, \varepsilon) A(\varepsilon, -\chi)| = 0, \end{aligned} \quad (25)$$

where

$$A(\varepsilon, \chi) = \begin{pmatrix} a_1 \sigma_2 e^{i\chi/2} & 0 \\ 0 & a_2 \sigma_2 e^{-i\chi/2} \end{pmatrix}, \quad (26)$$

and  $\mathcal{S}(\mathbf{p}_{\parallel}, \varepsilon)$ ,  $\underline{S}(\mathbf{p}_{\parallel}, \varepsilon)$  are effective electron and hole scattering matrices

$$\mathcal{S}(\mathbf{p}_{\parallel}, \varepsilon) = \begin{pmatrix} \mathcal{S}_{11}(\mathbf{p}_{\parallel}, \varepsilon) & \mathcal{S}_{12}(\mathbf{p}_{\parallel}, \varepsilon) \\ \mathcal{S}_{21}(\mathbf{p}_{\parallel}, \varepsilon) & \mathcal{S}_{22}(\mathbf{p}_{\parallel}, \varepsilon) \end{pmatrix}, \quad (27)$$

$$\underline{S}(\mathbf{p}_{\parallel}, \varepsilon) = \mathcal{S}^T(-\mathbf{p}_{\parallel}, -\varepsilon), \quad (28)$$

$$\mathcal{S}_{11}(\mathbf{p}_{\parallel}, \varepsilon) = S_{11} + q^{-4} e^{-i\varphi} S_{11'} (1 - q^{-4} e^{-i\varphi} S_{2'2}, S_{1'1'})^{-1} S_{2'2}, S_{1'1}, \quad (29)$$

$$\mathcal{S}_{12}(\mathbf{p}_{\parallel}, \varepsilon) = q^{-2} e^{-i\varphi/2} S_{11'} (1 - q^{-4} e^{-i\varphi} S_{2'2}, S_{1'1'})^{-1} S_{2'2}, \quad (30)$$

$$\mathcal{S}_{21}(\mathbf{p}_{\parallel}, \varepsilon) = q^{-2} e^{-i\varphi/2} S_{22'} (1 - q^{-4} e^{-i\varphi} S_{1'1'}, S_{2'2'})^{-1} S_{1'1'}, \quad (31)$$

$$\mathcal{S}_{22}(\mathbf{p}_{\parallel}, \varepsilon) = S_{22} + q^{-4} e^{-i\varphi} S_{22'} (1 - q^{-4} e^{-i\varphi} S_{1'1'}, S_{2'2'})^{-1} S_{1'1'}, S_{2'2} \quad (32)$$

The functions  $P(\varepsilon, \mathbf{p}_{\parallel}, \chi)$  and  $P_1(\varepsilon, \mathbf{p}_{\parallel}, \chi)$  are proportional to each other with the  $\chi$ -independent proportionality factor. The matrices  $\mathcal{S}(\mathbf{p}_{\parallel}, \varepsilon)$  and  $\underline{\mathcal{S}}(\mathbf{p}_{\parallel}, \varepsilon)$  describe normal state properties of our device while superconductivity is accounted for by the matrix  $A(\varepsilon, \chi)$  which depends on superconducting order parameters  $\Delta_{1,2}$  and the phase difference  $\chi$ .

#### IV. JOSEPHSON CURRENT: GENERAL EXPRESSIONS

It turns out that the function  $P(\varepsilon, \mathbf{p}_{\parallel}, \chi)$  (24) can be directly used in order to derive a general and compact expression for the Josephson current across SNS structure under consideration. In order to accomplish this task we will use the standard Green function formalism<sup>17</sup>. The corresponding derivation is presented in Appendix A. It yields the following result

$$I(\chi) = -2eAT \sum_{\omega_n > 0} \int_{|\mathbf{p}_{\parallel}| < p_F} \frac{d^2 p_{\parallel}}{(2\pi)^2} \frac{\partial P(i\omega_n, \mathbf{p}_{\parallel}, \chi) / \partial \chi}{P(i\omega_n, \mathbf{p}_{\parallel}, \chi)}, \quad (33)$$

where  $\omega_n = \pi T(2n + 1)$  is Matsubara frequency. Using standard transformation summation over Matsubara frequencies in Eq. (33) can be rewritten in terms of the integral

$$I(\chi) = -\frac{eA}{2\pi} \int d\varepsilon \tanh \frac{\varepsilon}{2T} \times \int_{|\mathbf{p}_{\parallel}| < p_F} \frac{d^2 p_{\parallel}}{(2\pi)^2} \text{Im} \frac{\partial P(\varepsilon, \mathbf{p}_{\parallel}, \chi) / \partial \chi}{P(\varepsilon + i0, \mathbf{p}_{\parallel}, \chi)}. \quad (34)$$

At energies close to the bound state  $P$  becomes a linear function of the energy variable,  $P(\varepsilon, \mathbf{p}_{\parallel}, \chi) \propto (\varepsilon - \varepsilon_B(\mathbf{p}_{\parallel}, \chi))$ . With this in mind one can easily check that Eq. (34) correctly describes the contribution from Andreev bound states. In Appendix A we also demonstrate that Eqs. (33) and (34) properly account for the scattering states contribution to  $I(\chi)$ . We can also add that momentum integration in Eqs. (33), (34) can be transformed into the sum over conducting channels

$$A \int_{|\mathbf{p}_{\parallel}| < p_F} \frac{d^2 p_{\parallel}}{(2\pi)^2} \rightarrow \sum_k. \quad (35)$$

The above expressions for  $I(\chi)$  define the Josephson current in SNS junctions with spin-active interfaces under very general conditions. In various physical situations underlying symmetries of the model typically limit the number of parameters of the scattering matrices  $\mathcal{S}_{1,2}$ . One important example was considered in Ref. 11 where we analyzed the Josephson current across a half-metallic layer in-between two superconducting electrodes. In that case one needs to assume that spin-active interfaces do not possess inversion symmetry<sup>9,11</sup> thus allowing for spin-flip scattering. Substituting the particular form of the scattering matrix<sup>11</sup> into the general expressions for  $I(\chi)$  derived here one immediately recovers the results<sup>11</sup>.

In this paper we consider another generic type of the scattering matrix describing spin-active interfaces which do possess inversion symmetry as well as reflection symmetry in the plane normal to the corresponding interface. Such  $\mathcal{S}$ -matrices can be chosen in the following form

$$S_{11} = S_{1'1'} = \underline{S}_{11}^T = \underline{S}_{1'1'}^T = U(\alpha) \begin{pmatrix} \sqrt{R_{1\uparrow}} e^{i\theta_{1/2}} & 0 \\ 0 & \sqrt{R_{1\downarrow}} e^{-i\theta_{1/2}} \end{pmatrix} e^{i\zeta_1} U^+(\alpha), \quad (36)$$

$$S_{11'} = S_{1'1} = \underline{S}_{11'}^T = \underline{S}_{1'1}^T = U(\alpha) i \begin{pmatrix} \sqrt{D_{1\uparrow}} e^{i\theta_{1/2}} & 0 \\ 0 & \sqrt{D_{1\downarrow}} e^{-i\theta_{1/2}} \end{pmatrix} e^{i\zeta_1} U^+(\alpha), \quad (37)$$

$$S_{22} = S_{2'2'} = \underline{S}_{22} = \underline{S}_{2'2'} = \begin{pmatrix} \sqrt{R_{2\uparrow}} e^{i\theta_{2/2}} & 0 \\ 0 & \sqrt{R_{2\downarrow}} e^{-i\theta_{2/2}} \end{pmatrix} e^{i\zeta_2}, \quad (38)$$

$$S_{22'} = S_{2'2} = \underline{S}_{22'} = \underline{S}_{2'2} = i \begin{pmatrix} \sqrt{D_{2\uparrow}} e^{i\theta_{2/2}} & 0 \\ 0 & \sqrt{D_{2\downarrow}} e^{-i\theta_{2/2}} \end{pmatrix} e^{i\zeta_2}. \quad (39)$$

Here  $R_{1(2)\uparrow(\downarrow)} = 1 - D_{1(2)\uparrow(\downarrow)}$  are spin dependent reflection coefficients of both NS interfaces,  $\theta_{1,2}$  are spin-mixing angles,  $\zeta_{1,2}$  are real phase parameters and  $U(\alpha)$  is the rotation matrix in the spin space which depends on the angle  $\alpha$  between polarizations of the two interfaces,

$$U(\alpha) = \exp(-i\alpha\sigma_1/2) = \begin{pmatrix} \cos(\alpha/2) & -i \sin(\alpha/2) \\ -i \sin(\alpha/2) & \cos(\alpha/2) \end{pmatrix}. \quad (40)$$

We would like to emphasize that – in contrast to the case studied in Refs. 9,11 – the scattering matrices (36)-(40) conserve the projection of the electron spin along the interface polarization axis and *do not* allow for spin-flip scattering.

Let us evaluate both the function  $P(\varepsilon, \mathbf{p}_{\parallel}, \chi)$  and the Josephson current in the case of non-collinear barriers po-

larizations. Absorbing the phases  $\zeta_{1,2}$  into the kinematic phase

$$\varphi = -2p_F x d - \zeta_1 - \zeta_2, \quad (41)$$

after some algebra we obtain

$$P(\varepsilon, \mathbf{p}_{\parallel}, \chi) = \left\{ [\cos \chi + W(D_{1\uparrow}, D_{1\downarrow}, \theta_1, D_{2\uparrow}, D_{2\downarrow}, \theta_2, \varepsilon)] [\cos \chi + W^*(D_{1\uparrow}, D_{1\downarrow}, \theta_1, D_{2\uparrow}, D_{2\downarrow}, \theta_2, -\varepsilon)] \cos^2(\alpha/2) + [\cos \chi + W(D_{1\downarrow}, D_{1\uparrow}, -\theta_1, D_{2\uparrow}, D_{2\downarrow}, \theta_2, \varepsilon)] [\cos \chi + W^*(D_{1\downarrow}, D_{1\uparrow}, -\theta_1, D_{2\uparrow}, D_{2\downarrow}, \theta_2, -\varepsilon)] \sin^2(\alpha/2) - \sin^2(\alpha/2) \cos^2(\alpha/2) \left( \left| \sqrt{R_{1\uparrow}} e^{i\theta_1/2} - \sqrt{R_{1\downarrow}} e^{-i\theta_1/2} \right|^2 (1 + a_1^2)^2 - 4a_1^2 \sin^2 \theta_1 \right) \times \left( \left| \sqrt{R_{2\uparrow}} e^{i\theta_2/2} - \sqrt{R_{2\downarrow}} e^{-i\theta_2/2} \right|^2 (1 + a_2^2)^2 - 4a_2^2 \sin^2 \theta_2 \right) \frac{1}{4a_1^4 D_{1\uparrow} D_{1\downarrow} D_{2\uparrow} D_{2\downarrow}} \right\}, \quad (42)$$

where

$$W(D_{1\uparrow}, D_{1\downarrow}, \theta_1, D_{2\uparrow}, D_{2\downarrow}, \theta_2, \varepsilon) = -\frac{1}{2a_1 a_2 \sqrt{D_{1\uparrow} D_{1\downarrow} D_{2\uparrow} D_{2\downarrow}}} \left\{ q^4 (e^{-i\theta_1} - a_1^2 \sqrt{R_{1\uparrow} R_{1\downarrow}}) (e^{-i\theta_2} - a_2^2 \sqrt{R_{2\uparrow} R_{2\downarrow}}) + q^{-4} (\sqrt{R_{1\uparrow} R_{1\downarrow}} - a_1^2 e^{i\theta_1}) (\sqrt{R_{2\uparrow} R_{2\downarrow}} - a_2^2 e^{i\theta_2}) - e^{-i\varphi} (\sqrt{R_{1\uparrow}} e^{-i\theta_1/2} - a_1^2 \sqrt{R_{1\downarrow}} e^{i\theta_1/2}) (\sqrt{R_{2\uparrow}} e^{-i\theta_2/2} - a_2^2 \sqrt{R_{2\downarrow}} e^{i\theta_2/2}) - e^{i\varphi} (\sqrt{R_{1\downarrow}} e^{-i\theta_1/2} - a_1^2 \sqrt{R_{1\uparrow}} e^{i\theta_1/2}) (\sqrt{R_{2\downarrow}} e^{-i\theta_2/2} - a_2^2 \sqrt{R_{2\uparrow}} e^{i\theta_2/2}) \right\}. \quad (43)$$

Eqs. (33), (42) and (43) fully determine the Josephson current in ballistic SNS junctions with spin-active interfaces and represent the central result of this paper. In the spin-isotropic limit this result reduces to that obtained in Ref. 18.

## V. JOSEPHSON CURRENT: SPECIFIC LIMITS

The above general expression for the Josephson current contains a lot of information which can be conveniently illustrated by considering specific limiting cases.

### A. Small spin-mixing angles

Lets us first analyze the limit of small spin-mixing angles  $\theta_1, \theta_2 \ll 1$ . In the tunneling limit ( $D_{1\uparrow}, D_{1\downarrow}, D_{2\uparrow}, D_{2\downarrow} \ll 1$ ) the expression for the Josephson current defined in Eqs. (33), (42) and (43) reduces

to a much simpler result

$$I(\chi) = -2eAT \sin \chi \sum_{\omega_n > 0} \int_{|p_{\parallel}| < p_F} \frac{d^2 p_{\parallel}}{(2\pi)^2} \times \text{Re} \frac{4a_1 a_2 \sqrt{D_{1\uparrow} D_{1\downarrow} D_{2\uparrow} D_{2\downarrow}}}{(1 - a_1^2)(1 - a_2^2)(q^4 + q^{-4} - 2 \cos \varphi)}. \quad (44)$$

This expression coincides with the result obtained in Ref. 18 for SINIS structures with effective spin-isotropic interface transmissions  $D_1 = \sqrt{D_{1\uparrow} D_{1\downarrow}}$  and  $D_2 = \sqrt{D_{2\uparrow} D_{2\downarrow}}$ .

In the opposite limit of the highly transparent interfaces  $R_{1\uparrow}, R_{1\downarrow}, R_{2\uparrow}, R_{2\downarrow} \ll 1$  and for small spin-mixing angles Eq. (33) reduces to the standard expression for the Josephson current in SNS structures with fully transparent interfaces<sup>19</sup>. Interestingly, the Josephson current turns out not to depend on the misorientation angle  $\alpha$  in both limits of weakly and highly transparent barriers at NS interfaces. At intermediate barrier transmissions the dependence of the supercurrent on the angle  $\alpha$  formally exists but remains very weak (see Figs. 2 and 3). It is also important to point out that no transition to the  $\pi$ -junction regime occurs in the limit of the zero spin-mixing angles.

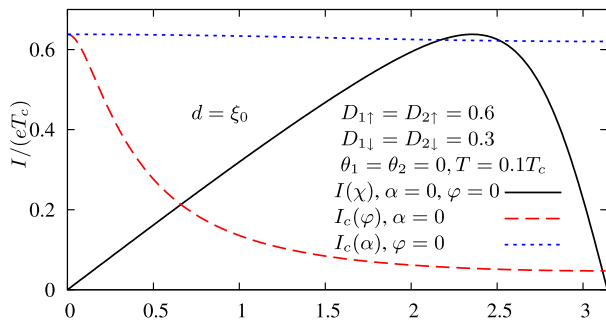


FIG. 2: Josephson current across single channel SNS junction with spin-active interfaces for  $d = \xi_0 = v_F/(2\pi T_c)$  and zero spin-mixing angles. The solid curve illustrates the current-phase relation, while dashed and dotted lines show the dependencies of the critical current respectively on the kinematic phase  $\varphi$  and on the misorientation angle  $\alpha$ .

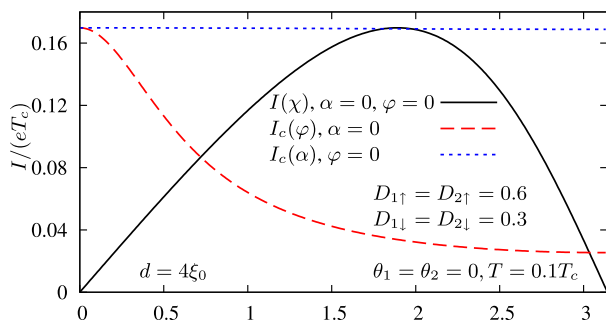


FIG. 3: The same as in Fig. 2 for  $d = 4\xi_0$ .

### B. Arbitrary spin-mixing angles

In a general case of arbitrary spin-mixing angles the junction behavior becomes much richer. In particular, the system may now undergo transitions between 0- and  $\pi$ -states driven by varying kinematic phase  $\varphi$ , misorientation angle  $\alpha$  and temperature. In Fig. 4 we present typical current-phase relations as well as the critical current dependence on the misorientation angle  $\alpha$ . We observe the  $\pi$ -to-0-junction transition occurs approximately at  $\alpha \approx 1.6$  for the chosen values of the parameters.

### C. Short junction limit

An important limiting case is realized provided the thickness of the normal layer tends to zero  $d \rightarrow 0$ . In

practice, this condition implies  $d \ll \xi_0$  off resonance, while at resonance this inequality turns out to be more stringent in the limit of small barrier transmissions<sup>18</sup>. In this short junction limit the general expression for the Josephson current becomes much simpler. For example, if the scattering matrix at the right interface is proportional to unity and  $|\Delta_1| = |\Delta_2| = \Delta$ , we recover the

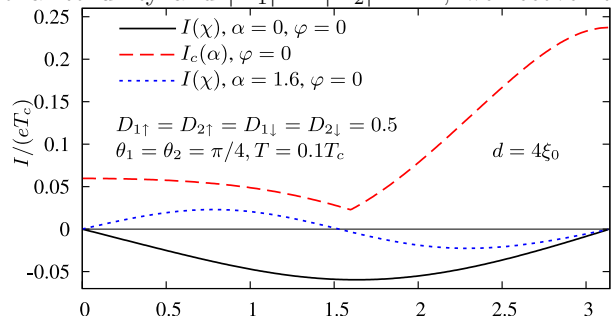


FIG. 4: The current-phase relation in single channel SNS junctions with spin-active interfaces for  $d = 4\xi_0$  and non-zero spin-mixing angles. Also the dependence of the critical current  $I_c$  on the misorientation angle  $\alpha$  is shown. The transition from  $\pi$ - to 0-junction regime occurs with increasing  $\alpha$ .

result of Barash and Bobkova<sup>20</sup>

$$I = \sum_k \frac{eD\Delta \sin \chi}{2\sqrt{1 - (\mathcal{R} + \mathcal{D} \cos \chi)^2}} \left[ \sin \Phi_+ \tanh \left( \frac{\Delta \cos \Phi_+}{2T} \right) - \sin \Phi_- \tanh \left( \frac{\Delta \cos \Phi_-}{2T} \right) \right], \quad (45)$$

where  $\mathcal{D} = \sqrt{D_{1\uparrow}D_{1\downarrow}}$ ,  $\mathcal{R} = \sqrt{R_{1\uparrow}R_{1\downarrow}}$  and

$$\Phi_{\pm} = \frac{\theta_1}{2} \pm \frac{1}{2} \arccos [\mathcal{R} + \mathcal{D} \cos \chi]. \quad (46)$$

Note, that in a general case one has  $\mathcal{R} + \mathcal{D} \neq 1$ . In the case of non-trivial scattering at the second collinear interface we again arrive at the Josephson current in the form (45), but obtain more complicated expressions for  $\mathcal{R}, \mathcal{D}, \Phi_{\pm}$

$$\mathcal{R} = \frac{\sqrt{R_{1\uparrow}R_{1\downarrow}} \cos \theta_2 + \sqrt{R_{2\uparrow}R_{2\downarrow}} \cos \theta_1 - \sqrt{R_{1\uparrow}R_{2\downarrow}} \cos((\theta_2 - \theta_1)/2 - \varphi) - \sqrt{R_{2\uparrow}R_{1\downarrow}} \cos((\theta_1 - \theta_2)/2 - \varphi)}{\sqrt{1 + R_{1\uparrow}R_{2\uparrow} - 2\sqrt{R_{1\uparrow}R_{2\uparrow}} \cos((\theta_1 + \theta_2)/2 - \varphi)} \sqrt{1 + R_{1\downarrow}R_{2\downarrow} - 2\sqrt{R_{1\downarrow}R_{2\downarrow}} \cos((\theta_1 + \theta_2)/2 + \varphi)}} \quad (47)$$

$$\mathcal{D} = \frac{\sqrt{D_{1\uparrow}D_{1\downarrow}D_{2\uparrow}D_{2\downarrow}}}{\sqrt{1 + R_{1\uparrow}R_{2\uparrow} - 2\sqrt{R_{1\uparrow}R_{2\uparrow}} \cos((\theta_1 + \theta_2)/2 - \varphi)} \sqrt{1 + R_{1\downarrow}R_{2\downarrow} - 2\sqrt{R_{1\downarrow}R_{2\downarrow}} \cos((\theta_1 + \theta_2)/2 + \varphi)}}.$$

As for  $\Phi_{\pm}$ , we should also substitute  $\theta_1$  in Eq.(46) by  $\theta$  given by

$$\theta = \arctan \frac{\sin(\theta_1 + \theta_2) - \sin((\theta_1 + \theta_2)/2 - \varphi) \sqrt{R_{1\downarrow}R_{2\downarrow}} - \sin((\theta_1 + \theta_2)/2 + \varphi) \sqrt{R_{1\uparrow}R_{2\uparrow}}}{\cos(\theta_1 + \theta_2) + \sqrt{R_{1\uparrow}R_{2\uparrow}R_{1\downarrow}R_{2\downarrow}} - \cos((\theta_1 + \theta_2)/2 - \varphi) \sqrt{R_{1\downarrow}R_{2\downarrow}} - \cos((\theta_1 + \theta_2)/2 + \varphi) \sqrt{R_{1\uparrow}R_{2\uparrow}}}. \quad (48)$$

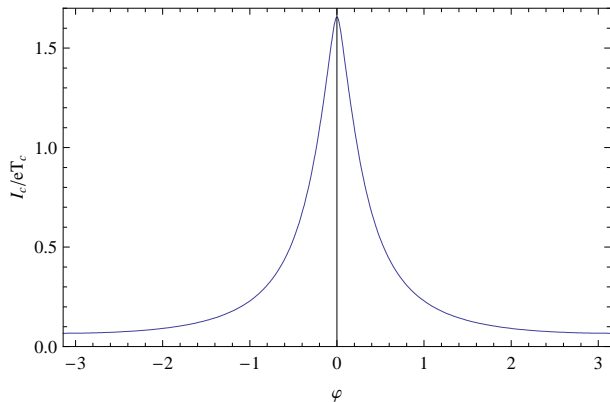


FIG. 5: The critical Josephson current for a short collinear ( $\alpha = 0$ ) single-channel SNS junction with  $D_{1\uparrow} = D_{2\uparrow} = 0.6, D_{1\downarrow} = D_{2\downarrow} = 0.3$  and  $\theta_{1,2} = 0$ . Here we have set  $T = 0.1T_c$ .

The last expression applies provided its denominator takes positive values, otherwise  $\pi$  should be added to the right-hand side of Eq. (48).

Current experimental techniques permit measuring Josephson current through junctions with few conducting channels formed, e.g. by single wall carbon nanotubes<sup>21,22,23</sup> or metallo-fullerenes<sup>24</sup>. In this case one can effectively tune the Josephson current by applying the gate voltage to the junction. This kind of measurements is essentially equivalent to detecting the  $\varphi$ -dependence of the supercurrent. Changing the gate voltage (or the phase  $\varphi$ ) one can drive the system towards resonance, thereby reaching substantial enhancement of the critical current. This resonance effect was experimentally demonstrated, e.g., in Ref. 21. In the case of SNS junctions with spin-active interfaces considered here the form of the resonant current peak becomes much more complicated. The corresponding examples are presented in Figs. 5, 6 and 7.

We observe that at zero spin-mixing angles  $\theta_{1,2}$  the form of the resonance peak is essentially identical to that for non-magnetic SNS junctions<sup>18</sup>, as demonstrated in

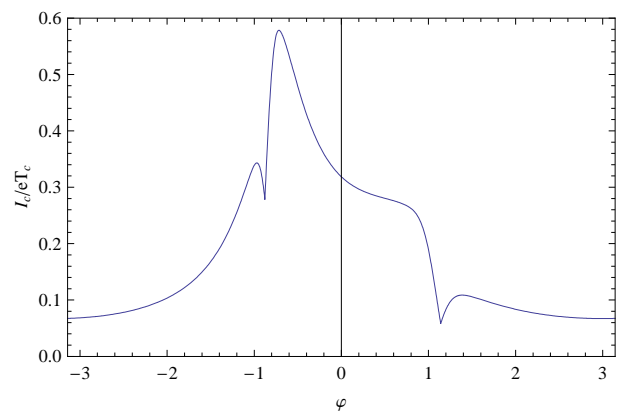


FIG. 6: The same as in Fig. 5 for  $\theta_1 = \theta_2 = \pi/4$ .

Fig. 5. The situation changes dramatically for non-zero values of the spin-mixing angles. In this case the resonant current peak in general becomes asymmetric and, on top of that, an additional dip structure emerges, see Fig. 6. It is important to emphasize that the current peak asymmetry is due to different spin-up and spin-down transmission values  $D_{\uparrow}$  and  $D_{\downarrow}$ . For equal values  $D_{\uparrow}$  and  $D_{\downarrow}$  the symmetry of the current peak is restored, however the peak now becomes split into two and also an additional dip structure remains as long as spin-mixing angles differ from zero, see Fig. 7. We also note that in the case of small barrier transmissions the current resonances are reached at the points  $\cos[(\theta_1 + \theta_2)/2 \pm \varphi] = 1$ .

The temperature dependence of the Josephson critical current for short SNS junctions is shown in the Fig. 8. It turns out that the temperature dependence can be non-monotonous even in the limit  $d \ll \xi_0$ . Note, however, that this non-monotonous behavior may occur only in the narrow range of  $\varphi$  in the vicinity of the local minimum of the  $I_c(\varphi)$ -dependence, cf. Figs. 6 and 7.

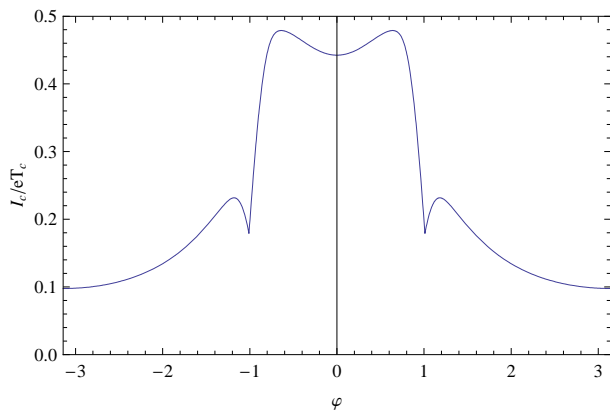


FIG. 7: The same as in Figs. 5 and 6 for  $D_{1\uparrow} = D_{2\uparrow} = D_{1\downarrow} = D_{2\downarrow} = 0.5$  and  $\theta_{1,2} = \pi/4$ .

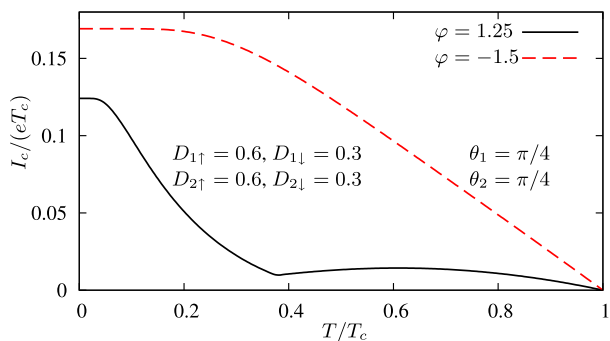


FIG. 8: The critical Josephson current for short collinear ( $\alpha = 0$ ) single channel SNS junctions as a function of temperature.

#### D. Long junctions at non-zero temperatures

In the limit of long junctions with  $d \gg v_F/T$  the result for the Josephson current simplifies dramatically and reads

$$I = 8eT \sin \chi \mathcal{A} \int_{|p_{\parallel}| < p_F} \frac{d^2 p_{\parallel}}{(2\pi)^2} \sqrt{D_{1\uparrow} D_{1\downarrow} D_{2\uparrow} D_{2\downarrow}} \times \exp(-2\pi T d / v_{Fx}) F, \quad (49)$$

where

$$F = \cos^2 \frac{\alpha}{2} \operatorname{Re} \left[ \frac{1}{(e^{i\theta_1} + \sqrt{R_{1\uparrow} R_{1\downarrow}}) (e^{i\theta_2} + \sqrt{R_{2\uparrow} R_{2\downarrow}})} \right] + \sin^2 \frac{\alpha}{2} \operatorname{Re} \left[ \frac{1}{(e^{-i\theta_1} + \sqrt{R_{1\uparrow} R_{1\downarrow}}) (e^{i\theta_2} + \sqrt{R_{2\uparrow} R_{2\downarrow}})} \right].$$

Note that even in this limit the above expression retains non-trivial features related to the presence of spin-active interfaces. In particular, for large enough values of the  $\theta$ -angles the  $\pi$ -junction behavior can be realized. Also, the transition between 0- and  $\pi$ -junction regimes can occur depending on the value  $\alpha$ . For example, in the case of

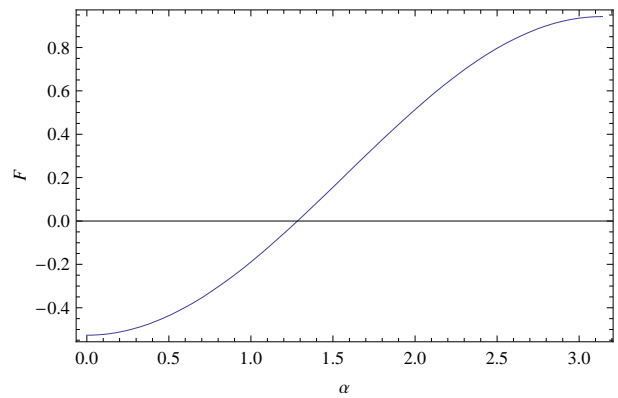


FIG. 9: The function  $F$  from Eq. (49) for identical interfaces with  $\sqrt{R_{\uparrow} R_{\downarrow}} = 0.9$  and  $\theta_{1,2} = 2.0$

identical weakly transmitting interfaces the  $\pi$ -junction regime is realized in the range  $\pi/2 < \theta_{1,2} < 3\pi/2$ . This behavior is demonstrated in Fig. 9. We observe that for smaller values of  $\alpha$  the function  $F(\alpha)$  takes negative values which corresponds to the  $\pi$ -junction regime. In contrast, for larger  $\alpha$  the function  $F(\alpha)$  becomes positive and the standard 0-junction regime is realized.

## VI. CONCLUDING REMARKS

In this paper we developed a general microscopic theory of dc Josephson effect in hybrid SNS structures with ballistic electrodes and spin-active NS interfaces. We evaluated the spectrum of Andreev levels (24) and derived a direct and simple relation between this spectrum and the Josephson current in such systems. The latter current can be expressed in a very compact general form (33) which contains complete information about non-trivial interplay between Andreev reflection and spin-dependent scattering at NS interfaces. Our analysis revealed a rich structure of properties realized in various physical limits. These properties – along with “usual” dependencies of the supercurrent on the junction size and temperature – also crucially depend on spin-dependent barrier transmissions, spin-mixing angles, relative magnetization orientation of interfaces as well as on the kinematic phase of scattered electrons.

In particular, we studied the current-phase relation in our system and demonstrated a broad range of different regimes including the presence of a  $\pi$ -junction state which may only be possible in the case of non-zero spin mixing angles. We also analyzed the effect of resonant enhancement of the critical current which mainly occurs in nanojunctions with few conducting channels driven by an externally applied gate voltage. We found that – in contrast to the non-magnetic case – spin-dependent scattering may dramatically modify both the magnitude and the shape of a resonant peak, e.g., making it asymmetric and/or providing an additional structure of dips, cf. Figs.



5, 6 and 7. We believe that these and other our predictions can be directly tested in experiments with hybrid superconducting-normal proximity structures containing, e.g. thin ferromagnetic layers. We also anticipate that further theoretical activity in the field might help to discover new exciting properties of the systems under consideration.

### Acknowledgments

This work was supported in part by RFBR grant 06-02-17459. M.S.K. also acknowledges support from the Dynasty Foundation.

### APPENDIX A: GREEN FUNCTIONS AND SUPERCURRENT

In order to derive the general expression for the Josephson current let us evaluate the Green functions  $G(x, x')$  for our system. Inside the normal metal and for  $d_1 < x < x' < d_2$  we have

$$G(x, x') = \begin{pmatrix} e^{i\varepsilon(x-d_1)/v_{Fx}} B_1^-(x') \\ e^{-i\varepsilon(x-d_1)/v_{Fx}} B_2^-(x') \end{pmatrix} e^{ip_{Fx}(x-d_1)} + \begin{pmatrix} e^{-i\varepsilon(x-d_1)/v_{Fx}} B_3^-(x') \\ e^{i\varepsilon(x-d_1)/v_{Fx}} B_4^-(x') \end{pmatrix} e^{-ip_{Fx}(x-d_1)}, \quad (\text{A1})$$

while for  $d_1 < x' < x < d_2$  we write

$$G(x, x') = \begin{pmatrix} e^{i\varepsilon(x-d_1)/v_{Fx}} B_1^+(x') \\ e^{-i\varepsilon(x-d_1)/v_{Fx}} B_2^+(x') \end{pmatrix} e^{ip_{Fx}(x-d_1)} + \begin{pmatrix} e^{-i\varepsilon(x-d_1)/v_{Fx}} B_3^+(x') \\ e^{i\varepsilon(x-d_1)/v_{Fx}} B_4^+(x') \end{pmatrix} e^{-ip_{Fx}(x-d_1)}, \quad (\text{A2})$$

where  $B_i^\pm(x)$  are  $2 \times 4$  matrices. The coefficients  $B_i^\pm(x)$  are determined from the relations

$$G(x, x+0) - G(x, x-0) = 0, \quad (\text{A3})$$

$$\left. \frac{\partial G(x, x')}{\partial x} \right|_{x'=x-0} - \left. \frac{\partial G(x, x')}{\partial x} \right|_{x'=x+0} = 2m\tau_3, \quad (\text{A4})$$

and interface boundary conditions (cf. Eqs. (19), (19))

$$\begin{pmatrix} B_1^-(x) \\ B_2^-(x) \end{pmatrix} = K_1 \begin{pmatrix} B_3^-(x) \\ B_4^-(x) \end{pmatrix}, \quad (\text{A5})$$

$$\begin{pmatrix} B_3^+(x) \\ B_4^+(x) \end{pmatrix} = e^{-i\varphi} Q K_2 Q \begin{pmatrix} B_1^+(x) \\ B_2^+(x) \end{pmatrix}. \quad (\text{A6})$$

Eqs. (A3) and (A4) yield

$$\begin{pmatrix} B_1^-(x) \\ B_2^-(x) \end{pmatrix} = \begin{pmatrix} B_1^+(x) \\ B_2^+(x) \end{pmatrix} + \frac{i}{v_{Fx}} \begin{pmatrix} T_1 e^{-i\varepsilon(x-d_1)/v_{Fx}} \\ -T_2 e^{i\varepsilon(x-d_1)/v_{Fx}} \end{pmatrix} e^{-ip_{Fx}(x-d_1)}, \quad (\text{A7})$$

$$\begin{pmatrix} B_3^-(x) \\ B_4^-(x) \end{pmatrix} = \begin{pmatrix} B_3^+(x) \\ B_4^+(x) \end{pmatrix} - \frac{i}{v_{Fx}} \begin{pmatrix} T_1 e^{i\varepsilon(x-d_1)/v_{Fx}} \\ -T_2 e^{-i\varepsilon(x-d_1)/v_{Fx}} \end{pmatrix} e^{ip_{Fx}(x-d_1)}, \quad (\text{A8})$$

where we introduced the matrices

$$T_1 = \begin{pmatrix} 1 & 0 & 0 & 0 \\ 0 & 1 & 0 & 0 \end{pmatrix}, \quad T_2 = \begin{pmatrix} 0 & 0 & 1 & 0 \\ 0 & 0 & 0 & 1 \end{pmatrix}, \quad (\text{A9})$$

Finally we obtain

$$\begin{pmatrix} B_1^+(x) \\ B_2^+(x) \end{pmatrix} = -\frac{i}{v_{Fx}} \left\{ (1 - e^{-i\varphi} K_1 Q K_2 Q)^{-1} K_1 \begin{pmatrix} T_1 e^{i\varepsilon(x-d_1)/v_{Fx}} \\ -T_2 e^{-i\varepsilon(x-d_1)/v_{Fx}} \end{pmatrix} e^{ip_{Fx}(x-d_1)} + (1 - e^{-i\varphi} K_1 Q K_2 Q)^{-1} \begin{pmatrix} T_1 e^{-i\varepsilon(x-d_1)/v_{Fx}} \\ -T_2 e^{i\varepsilon(x-d_1)/v_{Fx}} \end{pmatrix} e^{-ip_{Fx}(x-d_1)} \right\}, \quad (\text{A10})$$

$$\begin{pmatrix} B_3^+(x) \\ B_4^+(x) \end{pmatrix} = -\frac{i}{v_{Fx}} \left\{ (1 - e^{-i\varphi} Q K_2 Q K_1)^{-1} e^{-i\varphi} Q K_2 Q K_1 \begin{pmatrix} T_1 e^{i\varepsilon(x-d_1)/v_{Fx}} \\ -T_2 e^{-i\varepsilon(x-d_1)/v_{Fx}} \end{pmatrix} e^{ip_{Fx}(x-d_1)} + (1 - e^{i\varphi} Q K_2 Q K_1)^{-1} e^{-i\varphi} Q K_2 Q \begin{pmatrix} T_1 e^{-i\varepsilon(x-d_1)/v_{Fx}} \\ -T_2 e^{i\varepsilon(x-d_1)/v_{Fx}} \end{pmatrix} e^{-ip_{Fx}(x-d_1)} \right\} \quad (\text{A11})$$

Now we are ready to evaluate the Josephson current. Combining Eqs. (A1), (A2) and (A10), (A11) with the

general formula for the current

$$I = \frac{ieTA}{4m} \sum_{\omega_n > 0} \int_{|p_{\parallel}| < p_F} \frac{d^2 p_{\parallel}}{(2\pi)^2} \times \text{Sp} [(1 + \tau_3)(\nabla_{x'} - \nabla_x)_{x' \rightarrow x} G(x, x', i\omega_n)] \quad (\text{A12})$$

we arrive at the following expression

$$I(\chi) = -eAT \sum_{\omega_n > 0} \int_{|p_{\parallel}| < p_F} \frac{d^2 p_{\parallel}}{(2\pi)^2} \text{Im Sp} \left[ (1 + \tau_3) \times \left\{ (1 - e^{-i\varphi} K_1 Q K_2 Q)^{-1} - (1 - e^{-i\varphi} Q K_2 Q K_1)^{-1} \right\} \right]. \quad (\text{A13})$$

Making use of the identities

$$\frac{\partial K_1}{\partial \chi} = -\frac{i}{4} (\tau_3 K_1 - K_1 \tau_3), \quad (\text{A14})$$

$$\frac{\partial K_2}{\partial \chi} = \frac{i}{4} (\tau_3 K_2 - K_2 \tau_3), \quad (\text{A15})$$

$$\frac{\partial \det |A(t)|}{\partial t} = \text{Sp} [A^{-1}(t) A'_t(t)] \det |A(t)| \quad (\text{A16})$$

we verify the full equivalence of Eqs. (A13) and (33).

## APPENDIX B: CHANNEL-MIXING SCATTERING

Within our analysis we assumed that the electron momentum parallel to spin-active NS interfaces is conserved during scattering at such interfaces. This condition is equivalent to the absence of mixing between different transmission channels. The purpose of this appendix is to demonstrate that our approach can be straightforwardly generalized to the case of channel-mixing scattering.

Assume that there exist  $\mathcal{N}_N$  transmission channels in a normal metal layer, that can be scattered into  $\mathcal{N}_{S_1}$  and  $\mathcal{N}_{S_2}$  channels respectively in the left and right superconductors. The current amplitudes related via the scattering matrix will be numbered in the following order: spin-up current amplitudes at the left-hand side, spin-down current amplitudes at the left-hand side (ordered in the same way as spin-up amplitudes, i.e. for the same order of scattering channels), spin-up current amplitudes at the right-hand side and spin-down current amplitudes at the right-hand side. Thus, the block  $S_{11}$  describing electron reflection back into the left superconductor is given by the  $2\mathcal{N}_{S_1} \times 2\mathcal{N}_{S_1}$  matrix and  $S_{1'1'}$  block which accounts for electron reflection into the normal layer is presented by the  $2\mathcal{N}_N \times 2\mathcal{N}_N$  matrix. The blocks  $S_{11'}$ ,  $S_{1'1}$  are rectangular with dimensions  $2\mathcal{N}_{S_1} \times 2\mathcal{N}_N$  and  $2\mathcal{N}_N \times 2\mathcal{N}_{S_1}$  correspondingly. Hence, the total dimensions of the unitary matrix  $S_1$  are  $2(\mathcal{N}_{S_1} + \mathcal{N}_N) \times 2(\mathcal{N}_{S_1} + \mathcal{N}_N)$ .

The dimensions of blocks  $S_{22}$ ,  $S_{2'2'}$ ,  $S_{22'}$ , and  $S_{2'2}$  are  $2\mathcal{N}_N \times 2\mathcal{N}_N$ ,  $2\mathcal{N}_{S_2} \times 2\mathcal{N}_{S_2}$ ,  $2\mathcal{N}_N \times 2\mathcal{N}_{S_2}$ , and  $2\mathcal{N}_{S_2} \times 2\mathcal{N}_N$ . The blocks corresponding to the hole scattering matrices  $\underline{S}_{1,2}$  are characterized by the same dimensions. From the unitary scattering matrices  $S_1$  and  $\underline{S}_1$  we construct the  $4\mathcal{N}_N \times 4\mathcal{N}_N$  matrix

$$\check{M}_1 = \begin{pmatrix} \hat{e}_1 & \hat{f}_1 \\ \hat{g}_1 & \hat{h}_1 \end{pmatrix}. \quad (\text{B1})$$

The matrices  $\hat{e}_1, \hat{f}_1, \hat{g}_1, \hat{h}_1$  have dimensions  $2\mathcal{N}_N \times 2\mathcal{N}_N$  and are defined by

$$\begin{aligned} \hat{e}_1 &= (1 - \underline{S}_{1'1'} \underline{S}_{1'1'}^+)^{-1} \underline{S}_{1'1'} (-ia_1 \underline{S}_{11}^+ \hat{\sigma}_{y1} S_{11} + ia_1^{-1} \hat{\sigma}_{y1}) (1 - S_{11}^+ S_{11})^{-1} S_{1'1}^+, \\ \hat{f}_1 &= (1 - \underline{S}_{1'1'} \underline{S}_{1'1'}^+)^{-1} \underline{S}_{1'1'} (-ia_1 \underline{S}_{11}^+ \hat{\sigma}_{y1} + ia_1^{-1} \hat{\sigma}_{y1} S_{11}^+) (1 - S_{11} S_{11}^+)^{-1} S_{11'1}, \\ \hat{g}_1 &= -(1 - \underline{S}_{1'1'}^+ \underline{S}_{1'1'}^+)^{-1} \underline{S}_{11'1}^+ (-ia_1 \hat{\sigma}_{y1} S_{11} + ia_1^{-1} \underline{S}_{11} \hat{\sigma}_{y1}) (1 - S_{11}^+ S_{11})^{-1} S_{1'1}^+, \\ \hat{h}_1 &= -(1 - \underline{S}_{1'1'}^+ \underline{S}_{1'1'}^+)^{-1} \underline{S}_{11'1}^+ (-ia_1 \hat{\sigma}_{y1} + ia_1^{-1} \underline{S}_{11} \hat{\sigma}_{y1} S_{11}^+) (1 - S_{11} S_{11}^+)^{-1} S_{11'1}. \end{aligned} \quad (\text{B2})$$

Similarly, the unitary matrices  $S_2, \underline{S}_2$  describing electron scattering at the right interface are defined by

$$\begin{aligned} \hat{e}_2 &= (1 - \underline{S}_{22} \underline{S}_{22}^+)^{-1} \underline{S}_{22'} (-ia_2 \underline{S}_{2'2'}^+ \hat{\sigma}_{y2} S_{2'2'} + ia_2^{-1} \hat{\sigma}_{y2}) (1 - S_{2'2'}^+ S_{2'2'})^{-1} S_{22'}^+, \\ \hat{f}_2 &= (1 - \underline{S}_{22} \underline{S}_{22}^+)^{-1} \underline{S}_{22'} (-ia_2 \underline{S}_{2'2'}^+ \hat{\sigma}_{y2} + ia_2^{-1} \hat{\sigma}_{y2} S_{2'2'}^+) (1 - S_{2'2'} S_{2'2'}^+)^{-1} S_{2'2}, \\ \hat{g}_2 &= -(1 - \underline{S}_{22}^+ \underline{S}_{22}^+)^{-1} \underline{S}_{2'2}^+ (-ia_2 \hat{\sigma}_{y2} S_{2'2'} + ia_2^{-1} \underline{S}_{2'2'} \hat{\sigma}_{y2}) (1 - S_{2'2'}^+ S_{2'2'})^{-1} S_{22'}^+, \\ \hat{h}_2 &= -(1 - \underline{S}_{22}^+ \underline{S}_{22}^+)^{-1} \underline{S}_{2'2}^+ (-ia_2 \hat{\sigma}_{y2} + ia_2^{-1} \underline{S}_{2'2'} \hat{\sigma}_{y2} S_{2'2'}^+) (1 - S_{2'2'} S_{2'2'}^+)^{-1} S_{2'2}. \end{aligned} \quad (\text{B3})$$

Comparing these expressions we note that the matrices which account for the second interface are obtained from ones for the first interface by substituting the indices  $1 \rightarrow 2$  and, in addition, by interchanging the indices with and without the primes. The matrices  $\hat{\sigma}_{y1,2}$  have the di-

mensions  $2\mathcal{N}_{S_{1,2}} \times 2\mathcal{N}_{S_{1,2}}$  and the following structure

$$\hat{\sigma}_y = i \begin{pmatrix} 0 & -\hat{1} \\ \hat{1} & 0 \end{pmatrix}, \quad (\text{B4})$$

where  $\hat{1}$  is the unity matrix. The dimensions of this



- B **77**, 045311 (2008).
- <sup>16</sup> A. Millis, D. Rainer, and J.A. Sauls, Phys. Rev. B **38** 4504 (1988).
- <sup>17</sup> A.A. Abrikosov, L.P. Gorkov, and I.Ye. Dzyaloshinski, *Quantum Field Theoretical Methods in Statistical Physics*, 2nd ed. (Pergamon, Oxford, 1965).
- <sup>18</sup> A.V. Galaktionov and A.D. Zaikin, Phys. Rev. B **65**, 184507 (2002).
- <sup>19</sup> C. Ishii, Progr. Theor. Phys. **44**, 1525 (1970); I.O. Kulik, Zh. Eksp. Theor. Fiz. **57**, 1745 (1969) [Sov. Phys. JETP **30**, 944 (1970)].
- <sup>20</sup> Yu.S. Barash and I.V. Bobkova, Phys. Rev. B **65**, 144502 (2002) .
- <sup>21</sup> P. Jarillo-Herrero, J.A. van Dam, and L.P. Kouwenhoven, Nature (London) **439**, 953 (2006).
- <sup>22</sup> H.I. Jorgensen, T. Novotny, K. Grove-Rasmussen, K. Flensberg, and P.E. Lindelof, Nano Lett. **7**, 2441 (2007).
- <sup>23</sup> A. Eichler, R. Deblock, M. Weiss, C. Karrasch, V. Meden, C. Schoenenberger, and H. Bouchiat, arXiv:0810.1671.
- <sup>24</sup> H. Bouchiat, R. Deblock, S. Gueron, and A. Kasumov, unpublished.